Investigation of the Role and Mechanism of IF1 and STF1 Proteins, Twin Inhibitory Peptides Which Interact with the Yeast Mitochondrial ATP Synthase

ARTICLE *in* BIOCHEMISTRY · JULY 2003

Impact Factor: 3.02 · DOI: 10.1021/bi034394t · Source: PubMed

6 AUTHORS, INCLUDING:

Brèthes Daniel
French National Centre for Scientific Research
69 PUBLICATIONS **1,569** CITATIONS

SEE PROFILE

Investigation of the Role and Mechanism of IF1 and STF1 Proteins, Twin Inhibitory Peptides Which Interact with the Yeast Mitochondrial ATP Synthase

Renée Venard,[‡] Daniel Brèthes,[§] Marie-France Giraud,[§] Jacques Vaillier,[§] Jean Velours,[§] and Francis Haraux*[,‡]

Service de Bioénergétique & CNRS-URA 2096, DBJC, CEA Saclay, F91191 Gif-sur-Yvette, France, and Institut de Biochimie et Génétique Cellulaires du CNRS, 1, rue Camille Saint-Saëns, F33077 Bordeaux, France

Received March 11, 2003; Revised Manuscript Received April 25, 2003

ABSTRACT: Inhibition of the yeast F_0F_1-ATP synthase by the regulatory peptides IF1 and STF1 was studied using intact mitochondria and submitochondrial particles from wild-type cells or from mutants lacking one or both peptides. In intact mitochondria, endogenous IF1 only inhibited uncoupled ATP hydrolysis and endogenous STF1 had no effect. Addition of alamethicin to mitochondria readily made the mitochondrial membranes permeable to nucleotides, and bypassed the kinetic control exerted on ATP hydrolysis by the substrate carriers. In addition, alamethicin made the regulatory peptides able to cross mitochondrial membranes. At pH 7.3, F_0F_1-ATPase, initially inactivated by either endogenous IF1 or endogenous STF1, was completely reactivated hours or minutes after alamethicin addition, respectively. Previous application of a membrane potential favored the release of endogenous IF1 and STF1. These observations showed that IF1 and STF1 can fully inhibit ATP hydrolysis at physiological concentrations and are sensitive to the same effectors. However, ATP synthase has a much lower affinity for STF1 than for IF1, as demonstrated by kinetic studies of ATPase inhibition in submitochondrial particles by externally added IF1 and STF1 at pHs ranging from 5.5 to 8.0. Our data do not support previously proposed effects of STF1, like the stabilization of the IF1−F_0F_1 complex or the replacement of IF1 on its binding site in the presence of the proton-motive force or at high pH, and raise the question of the conditions under which STF1 could regulate ATPase activity *in vivo*.

F_0F_1[1] proton ATPase (or ATP synthase), present in mitochondria, chloroplasts, and bacteria, drives ATP synthesis at the expense of a proton-motive force (pmf) generated by an electron transfer chain (*1*, *2*). This enzyme can be fragmented into two different subcomplexes named F_0 and F_1. The F_0 sector is essentially membranous and acts as a proton channel. The MF_1 moiety is a soluble $\alpha_3\beta_3\gamma\delta\epsilon$ entity, which retains the ability to hydrolyze ATP. ATP synthases are today considered rotary molecular motors composed of a stator and a rotor (*2*, *3*).

F_0F_1 proton ATPase is known to be deactivated in the absence of the pmf. This regulation involves an inhibitory peptide called IF1 (reviews in refs *4* and *5*). First isolated from animal mitochondria (*6*), IF1 was also found in plant (*7*) and yeast (*8*) mitochondria. IF1 is readily removed from the MF_0MF_1 complex, which gives an active ATPase. Animal IF1 was proposed to bind to the C-terminal domain of β interacting with γ (*9*), whereas yeast IF1 was proposed to bind close to the catalytic site (*10*). The minimal sequence(s) and critical residues of IF1 necessary for the inhibitory effect have been investigated (*11*−*16*).

The pmf favors the release of IF1 from ATP synthase (*4*, *17*−*23*) or, alternatively, shifts IF1 from an inhibitory to a noninhibitory position on the enzyme (*24*−*26*). In deenergized mitochondria, MgATP is essential for ATPase inhibition by IF1 (*6*, *23*, *27*−*32*). In yeast mitochondria, MgADP was proposed to facilitate the release of IF1 inhibition by the pmf (*33*). IF1 from different sources is active at low pH and inactive at high pH (*6*, *7*, *12*, *15*, *16*, *34*−*39*). In animal IF1, His49 plays a major role in the pH dependency of the inhibitory effect (*15*). This residue has no counterpart in yeast, but Glu21 could play a similar role (*16*). Bovine IF1 forms dimers and tetramers below and above pH 6.5, respectively, and it was proposed that the dimer would be the active form of IF1 (*40*, *41*). Besides, isolated MF_1 proved to be stabilized under a dimeric form by IF1 binding (*41*, *42*).

In yeast, two other peptides, STF1 and STF2, are involved in F_1-ATPase regulation (*43*−*46*). STF1 and yeast IF1 are 63 residues long, and their sequences are highly homologous (*44*). STF2 is 83 residues long, and its homology with IF1 and STF1 is poor (*46*). Unlike IF1, STF1 at a saturating

* To whom correspondence should be addressed. Telephone: 33 1 69089891. Fax: 33 1 69088717. E-mail: haraux@dsvidf.cea.fr.

‡ CEA Saclay.

§ Institut de Biochimie et Génétique Cellulaires du CNRS.

[1] Abbreviations: (M)F_0(M)F_1, (mitochondrial) ATP synthase complex; (M)F_0, membranous subcomplex of (mitochondrial) ATP synthase; (M)F_1, catalytic subcomplex of (mitochondrial) ATP synthase; IF1, inhibitor peptide of mitochondrial ATPase, product of the *INH1* gene; STF1, product of the *STF1* gene (named also "9 kDa protein"); STF2, product of the *STF2* gene (named also "15 kDa protein"); Δ*inh1*, Δ*stf1*, and Δ*inh1*Δ*stf1*, strains lacking the *INH1* gene, the *STF1* gene, and both genes, respectively; WT, wild-type; OSCP, oligomycin sensitivity-conferring protein; SMP, submitochondrial particles; $\Delta\psi$, membrane potential; ΔpH, transmembrane pH difference; pmf, proton-motive force or transmembrane electrochemical proton gradient; R123, rhodamine 123; BCECF, 2′,7′-bis(2-carboxyethyl)-5(6)-carboxyfluorescein; CCCP, carbonyl cyanide *m*-chlorophenylhydrazone; FCCP, carbonyl cyanide *p*-(trifluoromethoxy)phenylhydrazone; PMSF, phenylmethanesulfonyl fluoride; CATR, carboxyatractyloside; DCCD, dicyclohexylcarbodiimide; PEP, phosphoenolpyruvate; PK, pyruvate kinase; LDH, lactate dehydrogenase; SDS, sodium dodecyl sulfate; BSA, bovine serum albumin; HPLC, high-performance liquid chromatography.

10.1021/bi034394t CCC: $25.00
Published on Web 05/24/2003

concentration was considered by some authors to only partially inhibit ATPase activity, by 40−60% (*47*−*49*), whereas others obtained data indicating that STF1 could inhibit isolated MF_1 by almost 100% (*50*). It was proposed that isolated MF_1 could not simultaneously bind IF1 and STF1 (*47*), whereas MF_0MF_1 could, provided STF2 was present (*48*). In the latter case, the functional state of the enzyme, fully or partially inhibited, was suggested to depend on the first peptide to be bound (*48*). The role of STF1 is unknown despite several hypotheses (*44*, *47*, *48*, *50*−*52*) based on impressive biochemical work (*10*, *16*, *32*, *39*, *43*−*49*, *51*, *53*). It was recently postulated that a fourth peptide, homologous to STF2 and called STF3, could contribute to yeast ATPase regulation (*52*).

This paper is focused on the comparison between the twin peptides IF1 and STF1. Understanding their role in ATPase regulation actually requires investigations at different levels. In this work, we have used intact mitochondria from WT, Δ*inh1*, Δ*stf1*, and Δ*inh1*Δ*stf1* strains to study the role of these peptides under conditions not much different from those prevailing in whole cells. We have also used alamethicin to make the inner membrane permeable for nucleotides, and discovered that the pores formed by alamethicin molecules also allowed IF1 and STF1 to cross the membranes. This property was used to study the release of the inhibitory peptides from ATP synthase and to investigate the role of pmf in this process. Finally, time-resolved ATP hydrolysis experiments with SMP allowed us to measure the rate binding constant of IF1 and STF1 under well-defined conditions. The two peptides proved to behave quite similarly, except that ATP synthase has a much lower affinity for STF1 than for IF1. Our results do not support previous proposals about inhibitory and binding properties of STF1 and raise the question of its precise role *in vivo*.

EXPERIMENTAL PROCEDURES

Yeast Strains. Saccharomyces cerevisiae strain D273-10B/A/H/U (MATα, *met6*, *ura3*, *his3*) (*54*) was the wild-type strain. Mutants Δ*inh1* and Δ*stf1*, lacking the IF1 and STF1 peptide, respectively, and the double mutant Δ*inh1*Δ*stf1* were a generous gift from D. Mueller (Chicago, IL).

Isolation of Mitochondria. Cells were grown aerobically at 28 °C in a complete liquid medium containing 2% lactate as a carbon source (*55*) and harvested in exponential growth phase. Mitochondria were prepared from protoplasts (*56*). Proteins were titrated according to the method of Lowry et al. (*57*), in the presence of 5% SDS, using BSA as a standard. Mitochondria were used a few hours after preparation, or frozen as fast as possible, to avoid formation of crystalline ice, by throwing small drops of a mitochondrial suspension into liquid nitrogen. For thawing, a few beads of frozen mitochondria were put in a cold, thin-walled glass tube, and plunged immediately into hot water (85 °C). Just before the total fusion, the tube was plunged into an ice/water mixture. The duration of the thawing procedure did not exceed 5 s. Mitochondria that had been frozen and thawed had high uncoupled respiratory rates and good respiratory control (*33*).

Submitochondrial Particles. Mitochondria that had been frozen and thawed (30−50 μL) were 15-fold diluted either in 20 mM Tris-SO_4 (pH 8.5) to favor the release of regulatory peptides or in 20 mM maleic acid (pH 6.0) to preserve their binding. The sample was sonicated on ice using a W-225 R tip sonicator (Ultrasonics Inc.). Three 45 s cycles (output control 2, 60% duty cycle) separated by 2 min intervals were applied. Samples were stored on ice at least between 1 h and 1 day before use. Their ATPase activity was perfectly stable for 1−2 days.

Purification of IF1 from Yeast Cells. IF1 was purified from yeast by a procedure adapted from refs *58* and *59*. A crude extract was obtained by washing 500 g of baker yeast in 0.1% galactose, concentrating the cells by low-speed centrifugation, resuspending them in 1 M $(NH_4)_2SO_4$, and heating at 95 °C for 10 min. After centrifugation, the supernatant, adjusted at pH 7, was mixed with Dowex 50 and eluted with 1 M $(NH_4)_2SO_4$, with water, with 7 M urea, and finally with 0.1 M Tris-SO_4 and 7 M urea. The last eluate was precipitated with ethanol at −20 °C, resuspended in 20 mM sodium acetate (pH 5), injected on a Beckman TSK SP-5PW HPLC column (10 μm, 7.5 mm × 7.5 cm), and eluted with the same buffer on an NaCl gradient (flow rate of 5 mL/min). The fractions containing IF1 were pooled and concentrated by ethanol precipitation. Proteins were titrated (*60*) using the Micro BCA reagent kit from Pierce, and synthetic IF1 as a standard. Purified IF1 appeared as a single band after SDS−PAGE.

Immunodetection of IF1 and STF1. Mitochondria (0.1 mg/mL) were lysed with 0.5 volume of dissociation buffer [0.45 M Tris-HCl (pH 6.8), 50% (w/v) glycerol, 6% SDS, and 0.05% bromophenol blue]. Proteins were separated by SDS−PAGE (*61*), electrotransferred onto a nitrocellulose membrane (Membrane Protean BA83, 0.2 μm, from Schleicher and Schuell) (*62*), and probed with anti-γ (1:10000), anti-IF1 (1:10000), or anti-STF1 (1:5000) polyclonal antibodies prior to treatment with anti-rabbit IgG-conjugated horseradish peroxidase antibodies (Pierce) at a dilution of 1:10000. Western blots were revealed with the ECL reagent (Amersham International) and were either visualized after exposure on Hyperfilm (Amersham International) or quantified using the *Versadoc Imaging System* from Bio-Rad. Anti-IF1 and anti-STF1 antibodies were kindly provided by K. Tagawa (Osaka, Japan).

Simultaneous Measurements of ATP Hydrolysis and Membrane Potential. Fresly prepared mitochondria were diluted to 0.3 mg/mL in the reaction medium thermostated at 28 °C and containing 10 mM Tris-maleate (pH 6.8), 0.65 M sorbitol, 0.3 mM EGTA, and 3 mM potassium phosphate. A 30 s activation step was initiated by adding ethanol [1% (v/v) final concentration] and terminated by adding 0.3 mM KCN. ATP hydrolysis was started by adding 0.5 mM ATP. $\Delta\psi$ was monitored by the quenching of rhodamine 123 fluorescence (0.5 μM) using a λ_{exc} of 485 nm and a λ_{em} of 533 nm, and calculated (in volts) according to the method of Beauvoit et al. (*63*):

$$\Delta\psi = 0.215[(F - F')/F + 0.123] \quad (1)$$

where F is the fluorescence intensity measured in the presence of CCCP (3 μM) and F' is the fluorescence intensity at a given time. ATP hydrolysis activity was measured by HPLC as follows. At different times, 50 μL of the reaction medium was withdrawn and the reaction was stopped by addition of 50 μL of 10% (v/v) perchloric acid followed by centrifugation for 2 min at 10000*g*. Fifty microliters of the supernatant was neutralized by addition of 40 μL of 1 M

Tris and diluted 10 times in pure water. Twenty microliters of each sample was injected on a Supelcosil LC18-DB HPLC column (3 μm, 3.3 cm $\times$ 4.6 mm) and eluted at 0.5 mL/min with 0.1 M potassium phosphate buffer (pH 6.3) containing 20 mM tetra-*n*-butylammonium hydrogen sulfate and 12% (v/v) MetOH. Nucleotides were detected at 254 nm.

Respiration Measurements. To measure NADH oxidation, 1 mL of the medium consisting of 0.65 M mannitol, 20 mM Tris-maleate, 3 mM potassium phosphate (pH 7.3), 1 mM $MgCl_2$, 17 mM KCl, 1 mg/mL BSA, and 1 mM NADH was put into a spectrophotometric microcuvette, stirred, and thermostated (25 °C). Respiration was started by adding a small volume of mitochondria that has been frozen and thawed (final concentration of 50−80 μg of protein/mL). NADH oxidation was monitored at 340 nm (optical pathway, 0.4 cm). Oxygen consumption was measured under identical conditions in the 3 mL chamber of a Clark-type electrode, as described previously (*33*).

Time-Resolved ATP Hydrolysis Measurements. Mitochondria that had been frozen and thawed or SMP were assayed for ATP hydrolysis, at a protein concentration of 50−80 μg/mL (mitochondria) or 3−10 μg/mL (SMP). The assay medium contained 0.65 M mannitol, 20 mM Tris-maleate, 3 mM potassium phosphate (pH 6.0 or 7.3), 1 mM $MgCl_2$, 17 mM KCl, 1 mg/mL BSA, and 2 μM antimycin, unless otherwise indicated. The ATP-regenerating system (2 mM PEP, 0.4 or 1 mM NADH, 20 units/mL PK, and 50 units/mL LDH) was present from the beginning or added shortly before the ATP hydrolysis reaction was initiated, as indicated. The NADH absorbance (340 nm) was continuously monitored in a stirred and thermostated cuvette (25 °C). In the case of mitochondria, the volume was 1 mL, the optical pathway 0.4 cm, and the NADH concentration 1 mM. In the case of SMP, the volume was 3 mL, the optical pathway 1 cm, and the NADH concentration 0.4 mM. The ATPase reaction was initiated by injecting 1 mM MgATP into the cuvette. Other additions are indicated. The time response, checked by ADP additions, was ~5 s. Kinetic analysis of changes in ATPase activity was carried out as described in ref *64*, except that the direct spectrophotometric recording was used instead of the first derivative. First-order kinetics of inhibition by IF1 and STF1 were thus fitted to the function displayed in eq 2 (see the Results). Nonlinear least-squares minimization was carried out using the solver of Microsoft Excel.

Reagents and Peptides. ADP, ATP, PEP, LDH, and PK were from Roche-Boehringer Mannheim. Antimycin A, oligomycin, CCCP, FCCP, valinomycin, nigericin, and alamethicin were from Sigma and prepared as stock solutions in methanol. Rhodamine 123 was from Molecular Probes. All others chemicals were analytical grade from Sigma or Merck. CATR was a generous gift from G. Lauquin (Bordeaux, France). Synthetic IF1 and STF1 were purchased from Neosystem (Strasbourg, France). IF1 was 90% pure, and STF1 was 80% pure; their molecular masses were checked by mass spectroscopy. Overexpression of STF1 in *Escherichia coli* will be published elsewhere.

RESULTS

Effect of IF1 and STF1 Peptides on ATP Hydrolysis in Intact Mitochondria. It was previously shown that yeast mitochondria contain the same amounts of IF1 and STF1 (*65*). Figure 1 shows immunoblots revealing IF1 (Figure 1a), STF1 (Figure 1b), and the γ subunit, in mitochondria prepared from WT yeast and from mutants where *INH1*, *STF1*, or both genes were disrupted. As expected, Δ*inh1* and Δ*stf1* mitochondria lack IF1 and STF1, respectively, and Δ*inh1*Δ*stf1* mitochondria lack both peptides. Integration of the chemiluminescence signals measured with the imaging device (data not shown) showed that Δ*inh1* mitochondria contain approximately the same amount of STF1 as WT mitochondria and Δ*stf1* mitochondria the same amount of IF1 as WT mitochondria, with respect to the amount of the γ subunit. Table 1 displays the rate of ATP hydrolysis by intact mitochondria from the four strains, measured in the presence of an inhibitor of the respiratory chain. Without an uncoupler, this activity is comparable in WT and Δ*inh1* mitochondria. CCCP addition slows ATP hydrolysis by WT mitochondria and considerably accelerates ATP hydrolysis by Δ*inh1* mitochondria. Expectedly, ATP hydrolysis is

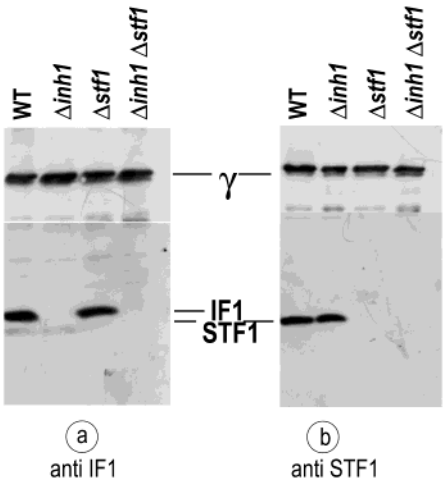

FIGURE 1: Immunodetection of IF1 and STF1 of mitochondrial lysates from WT, Δ*inh1*, Δ*stf1*, and Δ*inh1*Δ*stf1* strains. Mitochondrial proteins (20 μg) from each strain (mitochondria that had been frozen and thawed) were submitted to SDS−PAGE and Western blot analysis as indicated in Experimental Procedures: (a) detection using an antibody against IF1 and (b) detection using an antibody against STF1. Different lanes contained mitochondria from WT, Δ*inh1*, Δ*stf1*, and Δ*inh1*Δ*stf1* strains. Note that the antibody against IF1 also slightly reacts with STF1 (see also Figure 4).

Table 1: Rates of ATP Hydrolysis by Mitochondria Freshly Prepared from Various Strains[a]

		with CCCP	with DCCD	with CATR	with nigericin	with valinomycin
WT	41 ± 3	16 ± 3	14 ± 1	4 ± 1		
	44 ± 6	12 ± 3			45 ± 2	15 ± 2
Δ*inh1*	40 ± 5	400 ± 30	15 ± 1	0.2 ± 1		
Δ*stf1*	27 ± 2	9 ± 0.5	nd	nd		
Δ*inh1*Δ*stf1*	41 ± 5	365 ± 35	15 ± 1	2 ± 0.5		

[a] Conditions as described in Experimental Procedures. Values in nanomoles of ATP per milligram of protein per minute. Rates of ATP hydrolysis measured on mitochondria prepared from WT, Δ*inh1* (lacking IF1), Δ*stf1* (lacking 9 kDa protein), and Δ*inh1*Δ*stf1* (lacking both IF1 and 9 kDa protein) strains. CCCP (3 μM), nigericin (2 μM), valinomycin (80 μM), and CATR (2 μM) were added 5 s before ATP addition. DCCD (6 μg/mL) was added 15 s after ethanol addition and allowed to react for 1 min before KCN addition. For all experiments, ATP was added 1 min after KCN addition. Values are averages of at least two different experiments. The two rows with WT mitochondria refer to different preparations of mitochondria. nd means not determined.

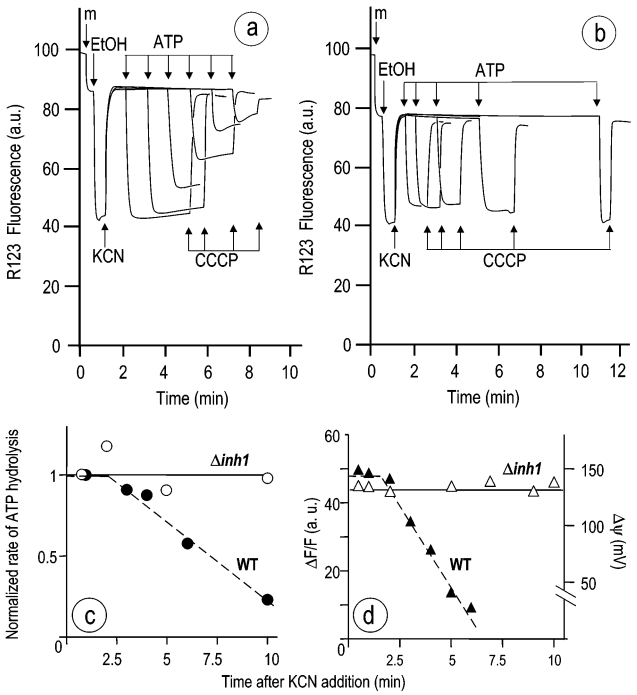

FIGURE 2: ATPase and proton pumping activities of MF_0MF_1 at different times after inhibition of the respiratory chain in WT and Δ*inh1* mitochondria. Conditions were as described in Experimental Procedures and Table 1. (a and b) Time course of the Δψ-dependent quenching of rhodamine 123 fluorescence. The different additions are indicated with arrows. m marks the addition of freshly prepared mitochondria. (a) Mitochondria from the WT strain. (b) Mitochondria from the Δ*inh1* strain. (c) Rate of ATP hydrolysis as a function of the time interval separating the addition of KCN and the addition of ATP, normalized to the activity measured after a 30 s time interval: (●) WT strain and (○) Δ*inh1* strain. (d) Maximal value of the energy-dependent quenching of rhodamine 123 fluorescence as a function of the time interval separating the addition of KCN and the addition of ATP. A scale of Δψ is given as an indication: (▲) WT strain and (△) Δ*inh1* strain.

inhibited by DCCD and CATR for both phenotypes. A comparison of WT, Δ*inh1*, and Δ*inh1*Δ*stf1* mitochondria shows that IF1 strongly inhibits ATP hydrolysis, as expected, but only with CCCP present. Without CCCP, the pmf generated by ATP hydrolysis probably minimizes the IF1 weight, by limiting the ATPase activity (back-pressure effect), and by moderating IF1 binding in WT mitochondria. It is also shown that Δ*stf1* mitochondria behave like WT mitochondria, and that Δ*inh1*Δ*stf1* mitochondria behave like Δ*inh1* mitochondria. Unlike IF1, the STF1 peptide, although present, has no effect here on ATPase activity.

ATP-Induced Membrane Potential in Intact Mitochondria. Figure 2 provides direct evidence of the process of self-maintaining ATPase activity in WT mitochondria, through measurement of the membrane potential Δψ by the quenching of R123 fluorescence. After a brief energization with ethanol as the respiratory substrate, leading to a decrease in the R123 fluorescence, the respiratory chain was inhibited by adding KCN, which resulted in a fast collapse of Δψ. ATP was added at various times after recovery of the maximal fluorescence, reached when Δψ dropped below the detection level. This ATP addition resulted in a new fluorescence decrease, due to the generation of Δψ by ATP hydrolysis. In WT mitochondria (Figure 2a), the extent of ATP-induced Δψ decreased when the time separating KCN and ATP additions was increased, but in Δ*inh1* mitochondria

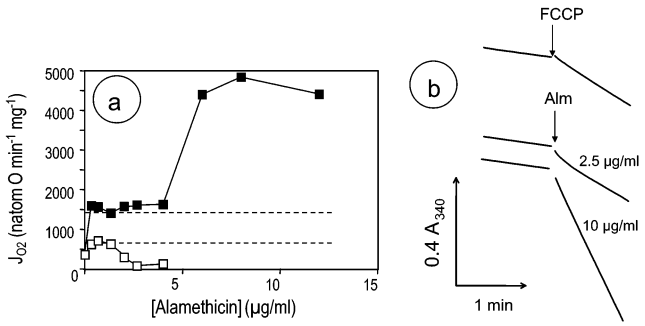

FIGURE 3: Effect of alamethicin on the respiratory activity of isolated mitochondria. Conditions were as described in Experimental Procedures. Mitochondria that had been frozen and thawed, at 25 °C and pH 7.3. (a) Rate of oxygen consumption as a function of alamethicin concentration: (■) NADH (1 mM), (□) ethanol (0.5%), and (- - -) levels obtained in the presence of FCCP (10 μM) and in the absence of alamethicin. (b) Time course of NADH oxidation by mitochondria, before and after addition of FCCP or alamethicin.

(Figure 2b), ATP-induced Δψ was constant and high. Panels c and d of Figure 2 show the ATPase activity and the magnitude of the resulting Δψ as a function of the time separating the additions of KCN and ATP. After the first Δψ collapse, WT mitochondria, but not Δ*inh1* mitochondria, progressively lose the ability to recover Δψ and ATPase activity upon addition of ATP. With respect to this property, mitochondria isolated from Δ*stf1* and Δ*inh1*Δ*stf1* mutants were comparable to those prepared from WT and Δ*inh1* strains, respectively (data not shown). This confirms the inhibitory role of IF1 and the lack of a detectable effect of the STF1 peptide in intact mitochondria.

The effect of the selective collapse of ΔpH (by adding nigericin) or Δψ (by adding valinomycin) on the self-maintained ATPase activity was studied in WT mitochondria. Valinomycin had the same effect as CCCP, and nigericin had no effect (Table 1). This indicates that the pmf generated by F_0F_1-ATPase prevents ATPase inhibition by IF1 through its Δψ component, and not through ΔpH or *via* the matrix alkalinization.

Effects of Alamethicin on Mitochondria. Because the interaction of IF1 is known to depend on a number of parameters which cannot be controlled in intact mitochondria, especially nucleotide and Mg^{2+} concentrations, we used alamethicin to create nonspecific pores through mitochondrial membranes (*66*) and better control the matrix content. Figure 3a shows the effect of alamethicin on the respiration rate of mitochondria in state 4, measured by oxygen consumption, with NADH or ethanol as the substrate. The rate of NADH oxidation (Figure 3a, filled symbols) is stimulated by alamethicin *via* a two-phase process. At low alamethicin concentrations (<1 μg/mL), the rate of NADH oxidation reaches the same level as that obtained in the presence of 10 μM FCCP, indicating an uncoupling effect increasing the activity of the NADH dehydrogenase located on the external face of the inner membrane. Beyond 4 μg/mL alamethicin, the oxidation rate increases again, to reach a second plateau. This second phase is due to the permeation of the mitochondrial inner membrane to NADH (*67*), revealing the activity of the internal NADH dehydrogenase. This interpretation was confirmed by studying the effect of alamethicin on the rate of ethanol oxidation through the endogenous NADH pool (Figure 3a, empty symbols). The respiration rate was

stimulated by low concentrations of alamethicin, and reached the same level as in the presence of FCCP, as in the case of NADH oxidation. At >2 μg/mL alamethicin, the oxidation rate dramatically decreases and falls to zero, as expected if the matricial NADH pool has been lost. The effect of alamethicin on the rate of NADH oxidation was found to be identical when the respiration rate was spectrophotometrically measured by the absorbance at 340 nm (not shown). Spectrophotometric recordings show that the increase in the rate of respiration upon alamethicin addition occurs in less than 5 s (Figure 3b).

These results demonstrate that alamethicin addition at concentrations of >6−8 μg/mL immediately makes the inner mitochondrial membrane highly permeable to NADH. Alamethicin also considerably increased the rate of ATP hydrolysis by FCCP-uncoupled mitochondria prepared from the Δ*inh1*Δ*stf1* strain, from 600−1000 to 4000−5000 nmol of ATP (mg of protein)$^{-1}$ min^{-1}, and made it CATR-resistant (not shown). This shows that in Δ*inh1*Δ*stf1* uncoupled mitochondria, ATP hydrolysis is kinetically controlled by the nucleotide or phosphate carriers, the substrate fluxes through alamethicin pores bypassing this control. On the other hand, increasing the time of incubation with alamethicin (10 or 20 μg/mL) to 1 h had only a slight effect on the respiration rate (10 and 20% decrease, respectively; data not shown), indicating that the organization of the respiratory chain was preserved. Alamethicin-treated mitochondria appear to be suitable for studying ATP hydrolysis by F_0F_1 in its native membrane, without kinetic limitation by the substrate carriers.

Alamethicin-Induced Permeability of the Mitochondrial Membranes to the Regulatory Peptides IF1 and STF1. Figure 4a, trace 1, shows the time course of ATP hydrolysis, coupled to NADH oxidation, by deenergized mitochondria prepared from WT cells and preincubated at pH 7.3. The activity is initially low and is somewhat stimulated after addition of 10 μg/mL alamethicin. Curve 2 shows that when alamethicin has been added to mitochondria some minutes before MgATP, a higher ATPase activity is observed, confirming that this activity progressively increases in the presence of alamethicin. Curve 3 shows that with Δ*inh1*Δ*stf1* mitochondria, the ATPase activity is very high as soon as alamethicin is added, and remains constant. It is therefore logical to ascribe the increase in ATPase activity of WT mitochondria to a progressive escape of the IF1 peptide through alamethicin pores. This interpretation is confirmed by the fact that pure IF1, externally added to Δ*inh1*Δ*stf1* mitochondria, inhibits the ATPase, but only when alamethicin is present (Figure 4a, curves 3 and 4).

To verify that IF1 does cross the pores created by alamethicin, we have centrifuged WT mitochondria, incubated them for 2 h in the medium used for kinetic experiments, in the presence or absence of 20 μg/mL alamethicin, and checked the pellet and the supernatant for the presence of IF1 and STF1 using Western blot analysis. The results are shown in Figure 4b. With mitochondria incubated in alamethicin-free medium, IF1 and STF1 were detected only in the pellet, at a level comparable to that found in noncentrifuged mitochondria. After alamethicin treatment, IF1 and STF1 were essentially found in the supernatant. Accordingly, ATPase activity, checked just before centrifugation, was 2400 nmol of ATP (mg of protein)$^{-1}$ min^{-1}f or the sample preincubated with alamethicin and only 350 nmol of ATP (mg of protein)$^{-1}$ min^{-1} for the control, supplemented with alamethicin immediately before measurement of the rate of ATP hydrolysis (data not shown).

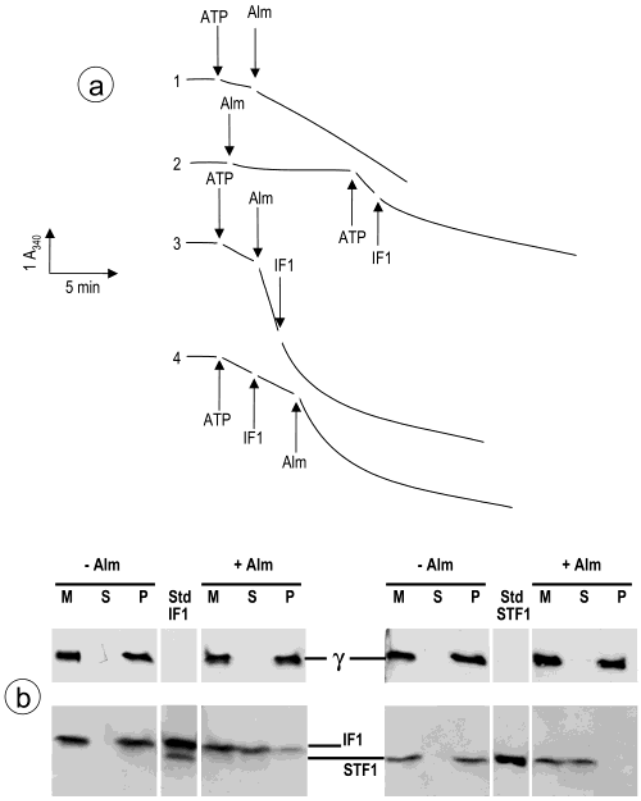

FIGURE 4: Time-dependent ATPase activation and inhibitor peptide release induced by adding alamethicin to mitochondria. Conditions were as described in Experimental Procedures. Mitochondria that had been frozen and thawed, at 25 °C and pH 7.3. (a) Time course of NADH oxidation coupled to ATP hydrolysis by WT (curves 1 and 2) and Δ*inh1*Δ*stf1* (curves 3 and 4) mitochondria. Different additions (1 mM MgATP, 10 μg/mL alamethicin, and 0.5 μM IF1) are denoted with arrows: curve 1, WT, MgATP added before alamethicin; curve 2, WT, MgATP added 10 min after alamethicin and 2 min before IF1; curve 3, Δ*inh1*Δ*stf1*, successive additions of MgATP, alamethicin, and IF1; and curve 4, Δ*inh1*Δ*stf1*, successive additions of MgATP, IF1, and alamethicin, showing no effect of IF1 unless alamethicin is added. (b) Immunodetection of IF1 and STF1 in the pellet and in the supernatant after centrifugation of wild-type mitochondria, treated or not treated with alamethicin. Mitochondria were diluted (0.1 mg of protein/mL) at 25 °C in the ATPase reaction medium (pH 7.3) devoid of NADH, PEP, and the PK/LDH mixture and supplemented with 1 mM PMSF. Samples were incubated for 5 min with FCCP (10 μM) and then further incubated under continuous stirring for 2 h, without (−Alm) or with (+Alm) alamethicin (20 μg/mL). Aliquots (2 mL) were then centrifuged for 15 min at 50000*g* (4 °C). Supernatants were taken up, and pellets were resuspended in 2 mL of the initial medium. Sixty microliters of each resulting sample was mixed with 30 μL of dissociation buffer and subjected to SDS−PAGE and immunoblotting as indicated in Experimental Procedures: (left) immunodetection using the anti-IF1 antibody and (right) immunodetection using the anti-STF1 antibody. Lanes M contained mitochondria before centrifugation, and lanes P and S contained pellet and supernatant, respectively, after centrifugation of mitochondria. Lanes Std IF1 and Std STF1 contained pure inhibitory peptides. The antibody against IF1 also slightly reacts with STF1 (left panel). Immunodetection of the γ subunit shows no release of F_1-ATPase in the supernatants.

We have studied the kinetics of activation of ATPase following the addition of alamethicin to mitochondria from

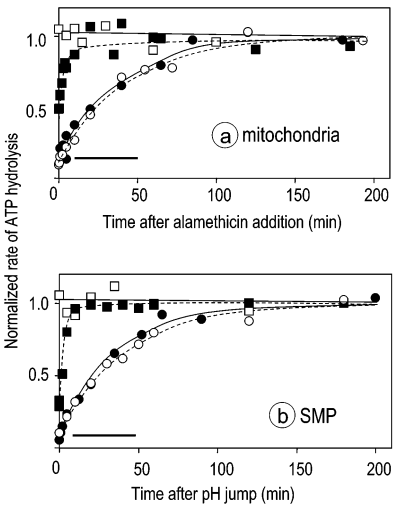

FIGURE 5: Time-dependent ATPase activation by addition of alamethicin to deenergized mitochondria (a) and by a fast pH increase in SMP (b). Conditions were as described in Experimental Procedures. (a) Rate of ATP hydrolysis as a function of the time separating addition of alamethicin (20 μg/mL) and addition of MgATP. Mitochondria that had been frozen and thawed from WT (●), Δ*inh1* (■), Δ*stf1* (○), and Δ*inh1*Δ*stf1* (□) strains. Maximal ATPase activities are 3900 (●), 3800 (■), 3100 (○), and 4500 nmol min^{-1} (mg of protein)$^{-1}$ (□). (b) Rate of ATP hydrolysis as a function of the time separating the pH jump (from 6 to 7.3) and addition of MgATP. SMP from WT (●), Δ*inh1* (■), Δ*stf1* (○), and Δ*inh1*Δ*stf1* (□) strains. Maximal ATPase activities are 3600 (●), 2000 (■), 2600 (○), and 1100 nmol min^{-1} (mg of protein)$^{-1}$ (□). Thick horizontal bars indicate the mean oligomycin-insensitive ATPase activity (practically independent of the strain).

WT, Δ*inh1*, Δ*stf1*, and Δ*inh1*Δ*stf1* strains (pH 7.3). Alamethicin (20 μg/mL) was added to antimycin-treated mitochondrial suspensions containing PEP and NADH. After a variable incubation time, a PK/LDH mixture was injected, and the ATPase reaction was initiated 15 s later by addition of MgATP. Figure 5a shows the rate of ATP hydrolysis as a function of the time separating alamethicin and MgATP additions. In WT mitochondria (●), ATPase is slowly activated due to inhibitor(s) release. The activity reaches a plateau after 2 h, half-activation occurring in ~25 min. The maximal ATPase activity was 85% inhibited by addition of exogenous IF1 or oligomycin (not shown). The residual 15% activity was not due to F_0F_1-ATPase. Comparison between initial and final activities in Figure 5a shows that initially, ATPase was more than 85% inhibited by endogenous peptides, and nearly 100% inhibited if one considers the oligomycin-sensitive activity. The pattern of activation is practically the same for Δ*stf1* mitochondria [Figure 5a (○)]. As expected, no time-dependent ATPase activation induced by alamethicin occurs in Δ*inh1*Δ*stf1* mitochondria [Figure 5a (□)]. In Δ*inh1* mitochondria, the ATPase activity increases rapidly after alamethicin addition [Figure 5a (■)]. Half-activation is reached in a few minutes. This increase in activity is likely due to the release of the STF1 inhibitory peptide, escaping through the alamethicin pores. Comparison between the initial and final activities shows that ATPase activity was initially inhibited by 50% (crude activity) or by 60% (oligomycin-sensitive activity).

pH-Dependent Release of IF1 and STF1 Peptides from Submitochondrial Particles. Kinetics of ATPase activation were also studied using nonenergized SMP submitted to an acid−base transition. SMP were prepared at pH 6.0 to keep the endogenous inhibitory peptides bound. Then, an aliquot of the SMP preparation was diluted in the reaction medium at pH 7.3 and 25 °C, and the ATPase reaction was initiated by addition of MgATP at various time after this pH jump. Figure 5b shows the ATPase activity as a function of the time separating the pH jump and MgATP addition. Kinetics of stimulation of the ATPase activity are quite similar to those obtained with alamethicin-treated mitochondria (compare panels a and b of Figure 5). As described previously, the apparent rate of peptide release is much higher for STF1 than for IF1 (compare the activation of Δ*inh1* and Δ*stf1* SMP). The initial inhibition by the endogenous peptides, deduced from the ratio between initial and final rates (Figure 5b), was ~90% for WT and Δ*stf1* strains and 70% for the Δ*inh1* strain (crude activities). It was 100 and 80%, respectively, for oligomycin-sensitive activities.

Kinetics of Inhibition of ATPase Activity of Submitochondrial Particles by Exogenous IF1 and STF1. From the results presented above, it is obvious that not only endogenous IF1 but also endogenous STF1 strongly inhibits ATP hydrolysis. At pH 7.3, the inhibition by endogenous STF1 is at least 70−80%. Because it is not possible to know if endogenous STF1 was at a saturating concentration, we have studied the kinetics of ATPase inhibition by exogenous IF1 and STF1 peptides, at pH 6.0. Experiments were carried out on SMP prepared as described previously, except that mitochondria were sonicated and stored at pH 8.5, to promote the dissociation of the inhibitory peptides, if any. SMP were then diluted in the assay medium at pH 6.0; MgATP was added, and a constant rate of ATP hydrolysis was immediately observed (Figure 6a). Finally, IF1 or STF1 was injected as a small volume of a concentrated solution preincubated at room temperature, and the rate of ATP hydrolysis immediately started to decrease. Figure 6a shows this decrease for two different concentrations of IF1. Since IF1 and STF1 are here in large excess with respect to ATP synthases, kinetics of ATP hydrolysis after IF1 (or STF1) addition could readily be fitted according to a simple model of pseudo-first-order decay, using the following equation:

$$y(t) - y_0 = V_\infty t + \left(\frac{V_0 - V_\infty}{k_{inh}}\right) e^{-k_{inh}t} \qquad (2)$$

where $y(t)$ is the NADH absorbance at 340 nm at time t after inhibitory peptide addition, y_0 the NADH absorbance at time zero, V_0 the initial rate of ATP hydrolysis and V_∞ the final rate of ATP hydrolysis (these rates being expressed in absorbance units per unit of time), and k_{inh} the apparent first-order rate constant of inhibition. If the inhibition is kinetically controlled by the binding of inhibitory peptide, k_{inh} obeys the following law:

$$k_{inh} = k_{on}[C] + k_{off} \qquad (3)$$

where k_{on} is the rate constant of binding (M^{-1} s^{-1}), [C] the peptide concentration in molarity, and k_{off} the rate constant of dissociation of the ATP synthase−peptide complex in inverse seconds. Figure 6b shows that k_{inh} is indeed proportional to the peptide concentration in the range that has been investigated (k_{off} is negligible here). It depends neither on the source of peptides (synthetic or natural IF1, synthetic or overexpressed STF1) nor on the phenotype of SMP (WT or

Table 2: Kinetics of ATPase Inhibition by IF1 Preincubated at Different pHs[a]

material	pH		IF1 concentration (μM)		percentage of inhibition	k_{inh} (s^{-1})
	incubation	assay	incubation	assay		
SMP	6	6	50	0.075	87.8	0.017 ± 0.002
SMP	7.3	6	50	0.075	88.5	0.017 ± 0.002
SMP	8	6	50	0.075	88.2	0.017 ± 0.002
MF_1	8.6	7	32	0.32	95.7	0.027 ± 0.003
MF_1	8.6	7	6.4	0.32	94.6	0.027 ± 0.003
MF_1	7	7	32	0.32	94.8	0.030 ± 0.003
MF_1	5.8	7	32	0.32	95.7	0.030 ± 0.003
MF_1	5.8	7	6.4	0.32	95.2	0.026 ± 0.003
MF_1	3.8	7	32	0.32	94.6	0.028 ± 0.003

[a] Conditions were as described in Experimental Procedures. IF1 was preincubated at various pHs (column 2) and checked by fast injection in the assay medium at a constant pH (column 3). Rows 1−3 are for experiments carried out using SMP prepared at pH 8.5 and assayed at pH 6. Rows 4−9 are for experiments carried out using purified MF_1, assayed at pH 7. In some cases (rows 4, 5, 7, and 8), the IF1 concentration was varied in the incubation medium (column 4), but its final concentration in the assay medium (column 5) was kept constant. The final percentage of inhibition (column 6) and the apparent inhibition rate constant k_{inh} (column 7) were determined using the same analysis as in Figure 6.

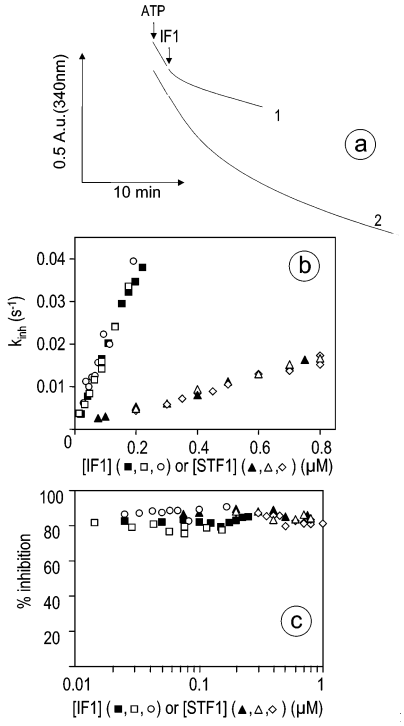

FIGURE 6: Kinetics of ATPase inhibition after addition of IF1 and STF1 peptides to SMP. Conditions were as described in Experimental Procedures (25 °C and pH 6). (a) Time course of NADH oxidation coupled to ATP hydrolysis: curve 1, addition of 125 nM IF1; and curve 2, addition of 25 nM IF1. (b) Rate constant of inhibition (k_{inh}) as a function of the concentration of synthetic IF1 (■ and □), natural IF1 (○), synthetic STF1 (▲ and △), and overexpressed STF1 (◇). SMP from WT (□, ○, and ◇) and Δ*inh1*Δ*stf1* (■, ▲, and △) strains. (c) Final percentage of ATPase inhibition as a function of IF1 concentration.

Δ*inh1*Δ*stf1*). The proportionality factor between the peptide concentration and k_{inh} gives here the following: $k_{on} = 1.8 \times 10^5$ M^{-1} s^{-1} for IF1 and $k_{on} = 2.4 \times 10^4$ M^{-1} s^{-1} for STF1 (mean values for peptides and SMP of all origins). In Figure 6c, the percentage of final inhibition of ATPase by IF1 or STF1 is plotted as a function of inhibitory peptide concentration. This percentage is constant for all the concentrations that were used, similar for IF1 and STF1, and comprised between 85 and 90%, the residual activity being oligomycin-resistant (not shown). Since full inhibition was reached for the lowest concentration of peptides that was used (25 nM for IF1 and 75 nM for STF1), the dissociation constants of the inhibitor−enzyme complexes are much lower than these values.

pH Dependency of the Interaction of IF1 and STF1 with ATP Synthase. It is well-known that IF1 is active at low pH and inactive at high pH (*6*, *12*, *15*, *34*−*38*). More precisely, it was found that the inhibitory effect depended on the pH of the medium where IF1 was preincubated before its transfer to the assay medium (*37*, *39*), which suggests a slow pH-dependent conformational change of IF1. With yeast IF1, the effect of preincubation pH was mentioned in a single study (*39*), with a limited time resolution. We have therefore reinvestigated this effect using continuous ATPase activity measurement. IF1 was first incubated for at least 2 h at room temperature, in buffers adjusted to different pHs and checked again for pH after IF1 addition. Then, a small aliquot of IF1 was added to the assay medium (pH 6) containing IF1-free SMP or, alternatively, to the assay medium (pH 7) containing MF_1-ATPase purified according to the method described in ref *68*. The second protocol was chosen to more closely match the conditions of the former study on yeast IF1 (*39*). The subsequent decay of ATPase was continuously monitored in the same way as in Figure 6. With our time resolution (between 5 and 10 s), absolutely no difference could be detected between the kinetics of inhibition by IF1 preincubated at different pHs (curves not shown). The main data are summarized in Table 2, which shows that the pH of IF1 preincubation does not affect the rate of ATPase inhibition. This absence of an effect of the preincubation pH was observed regardless of the origin of IF1 (synthetic or purified from yeast), and was also observed with STF1 (data not shown).

We have investigated the rate of binding of IF1 and STF1 as a function of the pH of the assay medium. The results are displayed in Table 3. The binding rate constant k_{on} decreases with pH, for IF1 as for STF1. At any pH, IF1 binding is much faster than STF1 binding. We have also estimated the rates of dissociation k_{off} of IF1 and STF1, by continuously assessing the ATPase reactivation in SMP (from Δ*stf1* and Δ*inh1* strains, respectively), prepared at pH 6 and rapidly diluted in a medium with a higher pH (curves not shown). k_{off} could be estimated at pH ≥7. Table 3 shows that this apparent k_{off} increases with pH, for IF1 as for STF1, and that it is higher for IF1 than for STF1 whatever the pH. In all cases, STF1 binding is disfavored and its release appears to be favored with respect to IF1.

Table 3: Apparent Kinetic Parameters of Binding (k_{on}) and Release (k_{off}) of IF1 and STF1 at Different pHs[a]

pH	apparent k_{on} (M^{-1} s^{-1}) IF1	apparent k_{on} (M^{-1} s^{-1}) STF1	IF1/STF1 ratio	apparent k_{off} (s^{-1}) IF1	apparent k_{off} (s^{-1}) STF1	IF1/STF1 ratio
5.5	$(2.2 \pm 0.2) \times 10^5$	$(3.0 \pm 0.2) \times 10^4$	7.3	nd	nd	nd
6	$(2.1 \pm 0.2) \times 10^5$	$(2.8 \pm 0.3) \times 10^4$	7.5	nd	nd	nd
6.5	$(1.7 \pm 0.2) \times 10^5$	$(1.0 \pm 0.1) \times 10^4$	17	nm	nm	nd
7	$(1.1 \pm 0.1) \times 10^5$	$(2.0 \pm 0.2) \times 10^3$	55	$(5 \pm 0.5) \times 10^{-4}$	$(1.7 \pm 0.2) \times 10^{-3}$	0.3
7.5	$(5.3 \pm 0.3) \times 10^4$	$(1.1 \pm 0.2) \times 10^3$	48	$(9.5 \pm 0.8) \times 10^{-4}$	$(7.0 \pm 0.5) \times 10^{-3}$	0.14
8	$(4.9 \pm 0.3) \times 10^4$	$(1.6 \pm 0.2) \times 10^3$	31	$(2.1 \pm 0.3) \times 10^{-3}$	$(2.5 \pm 0.5) \times 10^{-2}$	0.08

[a] Conditions were as described in Experimental Procedures. All measurements were taken in the presence of 1 mM MgATP. k_{on} was determined from experiments similar to those depicted in Figure 6, using WT SMP prepared and stored at pH 8.5 before use. k_{off} was determined using SMP prepared and stored at pH 6 to preserve initial peptide binding. k_{off} was drawn from experiments in which the rate of ATP hydrolysis was continuously monitored after the particles had been diluted in the reaction medium at the indicated pH. STF1 release was studied using Δ*inh1* SMP, and IF1 release was studied using Δ*stf1* SMP. Column 4 gives the ratio of k_{on} (IF1) to k_{on} (STF1). Column 7 gives the ratio of k_{off} (IF1) to k_{off} (STF1). nd means not determined and nm not measurable (too low).

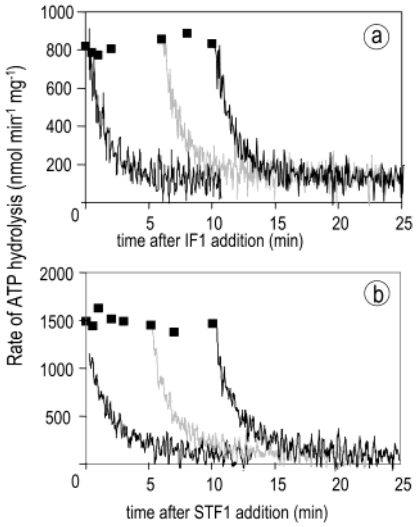

FIGURE 7: Effect of MgATP on the rate of ATPase deactivation by IF1 or STF1 added to SMP. Conditions were as described in Experimental Procedures. SMP prepared at pH 8.5 and assayed at pH 6 (25 °C). The continuous curves show the instantaneous rate of ATP hydrolysis as a function of the time following addition of 75 nM IF1 (a) or 500 nM STF1 (b). MgATP was added either before the peptide (left curves) or after the peptide (other curves), at times indicated by symbols (■). These curves are obtained from the first derivative of spectrophotometric recordings like those displayed in Figure 6a. The ordinate of symbols (■) gives the initial rate of ATP hydrolysis at the time where MgATP was injected. This rate was calculated by extrapolation using numerical analysis of the following first-order decay. Each symbol corresponds to a subsequent curve of the ATPase decay, but only three of these curves are represented on each plot, to avoid overlapping.

Effect of MgATP on the Interaction of IF1 and STF1 with ATP Synthase. It is established that ATP (or MgATP) is required for IF1 binding to ATPase (*6*, *23*, *27*−*32*). To know whether it is also needed for STF1 binding, we have studied the effect of MgATP on the rate of ATPase inhibition by IF1 and STF1, in experiments similar to that whose results are depicted in Figure 6a, with SMP prepared at pH 8.5 and assayed at pH 6. Figure 7 shows the rate of ATP hydrolysis as a function of the time after addition of IF1 (Figure 7a) or STF1 (Figure 7b). Continuous traces, which represent instantaneous rates of ATP hydrolysis, show the evolution of the ATPase activity in the presence of MgATP. There were drawn from the first derivative of spectrophotometric recordings. Symbols (■) represent the initial rates extrapolated to the time at which ATP was added, ATP being added either before IF1 (left kinetics) or at times indicated by squares (other kinetics). For clarity, only three kinetics are shown on each plot. For the other ones, the initial rate of ATP hydrolysis (■) is indicated. It can be seen that unless MgATP is added, there is no decrease in the ATPase activity due to IF1 or STF1. Like IF1, STF1 requires MgATP to bind the ATP synthase.

Role of the Proton-Motive Force in the Release of IF1 and STF1. While pmf is thought to favor the release of IF1 from ATP synthase (*4*, *17*−*23*), eventually by passing through a loosely bound, noninhibitory state of IF1 (*24*−*26*), its effect on the MF_1−STF1 interaction is not known. To answer this question, we have studied the pmf-induced ATPase activation in mitochondria from WT, Δ*inh1*, Δ*stf1*, and Δ*inh1*Δ*stf1* strains. The time schedule of experiments is displayed in Figure 8a. Mitochondria were incubated for 5 min at pH 7.3 either in the presence of NADH to generate pmf or in the presence of both FCCP and antimycin to collapse it. Then, alamethicin was added to allow the release of free inhibitory peptides, and after short times, MgATP was added to trigger ATP hydrolysis. Figure 8b shows, in the case of WT mitochondria, the initial rate of ATP hydrolysis as a function of the time separating the addition of alamethicin and the addition of MgATP. In initially deenergized mitochondria (■), only a low level of activation occurs within 1 min, as expected from the data depicted in Figure 5a. In preenergized mitochondria (●), a fast activation takes place, the maximum being practically reached when MgATP was added 30 s after alamethicin. This time-dependent activation can be interpreted as an efflux through the alamethicin pores of inhibitory peptide(s), made free by previous application of the pmf in the absence of MgATP. When MgATP is added, free peptides still present in the matrix immediately rebind, whereas peptides released outside mitochondria do not, due to dilution in the outer medium. Nigericin did not prevent this pmf-induced, alamethicin-revealed ATPase activation (○), which shows that pmf alone, even reduced to its electrical component, favors IF1 dissociation, and confirms the data of Table 1.

Experiments similar to that depicted in Figure 8b were carried out using mitochondria from the Δ*inh1* strain (Figure 8c), the Δ*stf1* strain (Figure 8d), and the Δ*inh1*Δ*stf1* strain (Figure 8e). Figure 8c shows that STF1 partially inhibits the ATPase activity in deenergized mitochondria, and is released from the enzyme by applying pmf. Δ*stf1* mitochondria behave like WT mitochondria (Figure 8d). As expected, the energetic state of mitochondria does not influence the

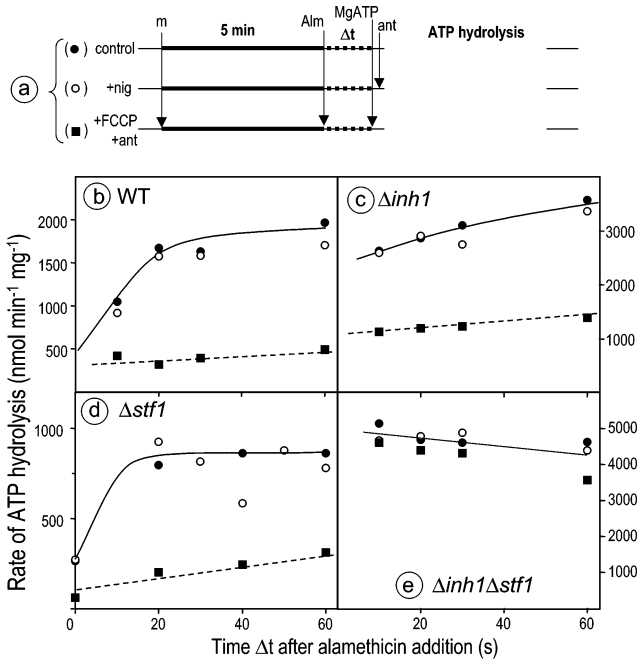

FIGURE 8: Effect of membrane energization on the ATPase activity in mitochondria measured under conditions of maximal turnover rate. Conditions as described in Experimental Procedures (25 °C and pH 7.3). (a) Time course of the experiments. Additions (m, mitochondria that had been frozen and thawed; Alm, 20 μg/mL alamethicin; and ant, antimycin) are indicated by vertical arrows: (●) control conditions, (○) nigericin (0.2 μM) initially present, and (■) FCCP (10 μM) and antimycin (5 μM) initially present. (b−e) Rates of ATP hydrolysis as a function of time Δt separating addition of alamethicin and addition of MgATP, in mitochondria from WT (b), Δ*inh1* (c), Δ*stf1* (d), and Δ*inh1*Δ*stf1* (e) strains.

ATPase activity in mitochondria from the Δ*inh1*Δ*stf1* strain (Figure 8e). These experiments show that pmf favors the release of both IF1 and STF1 peptides. From the ratios between the maximum and the minimum rates of ATP hydrolysis in panels b−d of Figure 8, it is deduced that under deenergized conditions, ATPase was inhibited by at least 85% in WT mitochondria, 60% in Δ*inh1* mitochondria, and 85% in Δ*stf1* mitochondria (values not corrected for the oligomycin-insensitive activities).

DISCUSSION

Comparison of Functional Properties of IF1 and STF1. Understanding the respective roles of IF1 and STF1 in ATPase regulation requires a comparison of their inhibitory properties and the modulation of these properties by the main known effectors: pH, nucleotides, and pmf.

We have shown that STF1 added to SMP at saturating concentrations inhibited the ATPase activity by practically 100%. In addition, experiments using alamethicin-treated mitochondria or SMP submitted to a pH jump have revealed that at pH 7.3, endogenous STF1 inhibits the oligomycin-sensitive ATPase activity by 60−80%. This degree of inhibition is certainly underestimated, due to the fast initial ATPase activation in the Δ*inh1* strain (see Figure 5). So STF1 must be considered a full inhibitor, like IF1.

Using deenergized SMP, we have investigated the effect of pH on the interaction between the ATP synthase and the two inhibitory peptides. When the pH is increased, the apparent k_{on} decreases and the apparent k_{off} increases (Table 3). The effect is still more pronounced for STF1 than for IF1. At any pH, STF1 binds much less rapidly than IF1 to ATP synthase and is released faster, so its affinity for the enzyme is always low compared to that of IF1.

Like IF1, STF1 requires MgATP to bind ATP synthase (Figure 7). This common feature strengthens the view according to which the basic mechanism of binding and inhibition is the same for the two peptides.

Experiments with mitochondria, in which energy-dependent peptide dissociation was revealed with alamethicin (Figure 8), have clearly shown that the membrane potential, already known to favor the dissociation of IF1 from ATP synthase, also favors STF1 dissociation.

To summarize, except for their affinity for the ATP synthase, the two peptides IF1 and STF1 have the same functional properties and are sensitive to the same effectors.

Comparison with Previous Data. At pH 6 (Figure 6) and pH 6.5 (not shown), we observed the maximal inhibition of ATPase activity from the lowest concentrations of IF1 and STF1, 25 and 75 nM, respectively. These results were obtained with SMP as well as with isolated MF_1. This means that the K_d value, too low to be estimated here, is in the nanomolar range, or even below, for both peptides. This is much lower than the K_d previously proposed (*47*) on the basis of binding experiments using gel filtration at pH 6.5 (~4 μM for IF1 and for STF1), but only slightly lower than the K_d value proposed in the early going by the same team for IF1 (11 nM) on the basis of activity measurements (*32*). We tend to favor activity measurements, because inhibitory peptides could have been partly released from MF_1-ATPase during the gel filtration step following binding experiments.

From our data, STF1 at saturating concentrations fully inhibits ATPase activity, which contradicts pioneering studies (*47*, *49*). This divergence is difficult to understand, but at least one possible explanation can be proposed. Early experiments were actually conducted in two steps: (1) incubation of concentrated MF_1-ATPase and STF1 at pH 6.5 in the presence of MgATP and (2) 50-fold dilution of the preparation in the assay medium at pH 7.3 (*47*). The second step lowered the maximal STF1 concentration to the micromolar range. At pH 7.3, this concentration was probably no more saturating (contrary to what happened at pH 6.5), and this could have significantly affected the activity measurement, the time resolution of which was not mentioned. Our kinetic data indeed show that at pH 7.3, STF1 release occurs in a few minutes. More recent studies, involving time-resolved assays, indicated that at pH 6.6, isolated MF_1-ATPase was almost fully inhibited by STF1 (*50*). Importantly, the study presented here shows that this feature does not depend on the biochemical state of the enzyme (isolated MF_1, whole complex in SMP, or alamethicin-treated mitochondria).

Contrary to previous investigators, we could not detect any effect of the preincubation pH on the functional properties of IF1 (Table 2). In the case of animal mitochondria, most experiments on the pH effect actually involved preincubation of IF1 mixed with MF_1 (*6*, *12*, *34*−*36*), and therefore, they do not discriminate between the effects on IF1 and the effects on the IF1−MF_1 complex. In one report, preincubation of free IF1 at various pHs revealed without ambiguity a slow transition (several tens of seconds) between protonated and deprotonated forms of IF1 (*37*). However,

such a transition took only a few seconds in ref *29*, which suggests that subtle parameters, not yet mastered, could control its rate. With plant IF1, an effect of the preincubation pH was observed in ref *7*, but not in ref *13*. The fact that IF1 was preincubated together with MF_1 in the first case, and alone in the second case, could explain the difference. In yeast, a slow pH-dependent transition, occurring in a few minutes, was mentioned in a single report (*39*), the only one which should be directly compared to the work presented here. When the time resolution of our experiments is taken into account, a transition occurring over a period of time longer than 5−10 s should have been detected. At present, we have no explanation for this discrepancy. Since traces of some divalent metals might affect the activity of IF1 (*69*), we checked the effect of preincubating IF1 in EDTA-containing buffers and saw no difference (data not shown). As indicated above, we also observed no difference between the synthetic peptide and the peptide purified from yeast.

IF1 and STF1 in Intact Mitochondria. In intact mitochondria from WT, Δ*inh1*, Δ*stf1*, and Δ*inh1*Δ*stf1* strains, the only differences in the patterns of ATP hydrolysis were due to the disruption of the *INH1* gene (Table 1). Disruption of the *STF1* gene had no measurable effect. Therefore, in intact mitochondria from WT and Δ*inh1* strains, the STF1 peptide is present (Figure 1), but silent under our conditions (Table 1). This is easy to understand in WT mitochondria, because IF1, which has the highest-affinity ATP synthase, is expected to be preferentially bound in the absence of pmf, and in the presence of pmf, both inhibitory peptides are presumably released. In the case of the Δ*inh1* strain, however, one may wonder why no inhibitory effect of STF1 could be detected in intact mitochondria, whereas it was revealed in SMP and alamethicin-treated mitochondria. In the absence of an uncoupler, the pmf generated by ATP hydrolysis keeps STF1 dissociated from the enzyme complex, because the affinity of STF1 for F_1-ATPase is low. However, in CCCP-treated mitochondria, where the pmf is theoretically collapsed, which was checked by the fluorescence of rhodamine 123 ($\Delta\psi$ component) and the fluorescence of BCECF (ΔpH component), STF1 is expected to inhibit ATP hydrolysis. This is not observed probably as a consequence of several additive factors. On one hand, in mitochondria uncoupled with CCCP, the strong kinetic control exerted by nucleotide and phosphate carriers certainly masks the inhibition of F_0F_1-ATPase, provided this inhibition is not total. On the other hand, it is conceivable that even in the presence of 3 μM CCCP, a residual ATPase-driven pmf, lower than the detection threshold, and possibly restricted to the close vicinity of ATP synthases, subsists and ensures the self-maintenance of some ATPase activity. All these factors minimizing and masking inhibition by STF1 disappear in the presence of alamethicin, which equilibrates the matrix with the external medium more drastically than CCCP does.

Previously Proposed Roles for STF1. STF1 was proposed to stabilize the ATP synthase−IF1 complex (*44*, *48*). Since IF1 and STF1 peptides are both full inhibitors, it is difficult to discriminate, from activity measurements, between the inhibitory effect of STF1 and its possible stabilizing effect on the IF1−ATPase complex. However, the stability of the complex between IF1 and the ATP synthase does not seem to depend on the presence of STF1, because the rates of ATPase activation are identical in material extracted from WT and Δ*stf1* cells (Figure 5).

It was also proposed that the STF1 peptide could replace IF1 on its binding site in the presence of a pmf, protecting ATP synthase from full inhibition (*47*, *51*). This proposal is not supported by the present view that the STF1 peptide, like IF1, is actually a full inhibitor. It is also inconsistent with the fact that pmf favors STF1 release as well as IF1 release.

Ultracentrifugation studies have indicated that at high pH, STF1 forms dimers more easily than at low pH, unlike yeast IF1 (*50*). Since the dimeric state of animal IF1 was previously proposed to be its only inhibitory form (*40*, *41*), it was suggested that STF1 could replace IF1 at high pH, where IF1 is not operative (*50*). This proposal is not satisfactory for different reasons. First, pH-dependent oligomerization is quite different for animal and yeast IF1, involving a dimer−tetramer equilibrium in the first case (*40*, *41*) and a monomer−dimer equilibrium in the second case (*50*). Second, these data indicate that at high pH, ATPase inhibition by STF1 is even more disfavored than inhibition by IF1 (Table 3). We also think that there is no evidence that monomeric forms of yeast IF1 and STF1 are not inhibitory. In our hands, ATPase inhibition by excess IF1 and STF1 always obeyed a first-order process (at concentrations ranging from 25 nM to 1 μM), which precludes any concentration-dependent change in their functional state during the kinetics of inhibition (more than 10 min). We also verified that the kinetics of ATPase inhibition by IF1 and STF1 at submicromolar concentrations were not affected by diluting the peptides in the reaction medium 4 h before the assay (data not shown). Finally, the existence of the dimeric form of endogenous yeast IF1 was recently questioned (*70*). Although we cannot ignore the question of IF1 and STF1 dimers, at present we have no evidence of their relevance in the inhibition process, and it seems unlikely that STF1 could replace IF1 at high pH. It remains possible, however, that STF1 could replace IF1 under some conditions not yet investigated, or could indirectly modify IF1 binding to ATP synthase, for example by forming hetero-oligomers.

ACKNOWLEDGMENT

Thanks are due to Gwénaëlle Moal for her excellent technical assistance and to Cécile Cartier for her help in experiments. Some kinetic experiments were carried out by Vincent Corvest during his license stay (Université Paris-Sud, centre d'Orsay, France). We are indebted to Pr. Michel Rigoulet for helpful discussions. Thanks are due to Dr. David Mueller for his gift of the Δ*inh1*, Δ*stf1*, and Δ*inh1*Δ*stf1* strains and to Professor Kunio Tagawa for the gift of antibodies against IF1 and STF1.

REFERENCES

1. Mitchell, P. (1961) *Nature 1*, 144−148.
2. Boyer, P. D. (1997) *Annu. Rev. Biochem. 66*, 717−749.
3. Engelbrecht, S., and Junge, W. (1997) *FEBS Lett. 414*, 485−491.
4. Schwerzmann, K., and Pedersen, P. L. (1986) *Arch. Biochem. Biophys. 250*, 1−18.
5. Green, D. W., and Grover, G. J. (2000) *Biochim. Biophys. Acta 1458*, 343−355.
6. Pullmann, M. E., and Monroy, G. C. (1963) *J. Biol. Chem. 238*, 3762−3768.
7. Norling, B., Tourikas, C., Hamasur, B., and Glaser, E. (1990) *Eur. J. Biochem. 188*, 247−252.

8. Matsubara, H., Hase, T., Hashimoto, T., and Tagawa, K. (1981) *J. Biochem. 90*, 1159−1165.
9. Jackson, P. J., and Harris, D. A. (1988) *FEBS Lett. 229*, 224−228.
10. Ichikawa, N., Yoshida, Y., Hashimoto, T., and Tagawa, K. (1996) *J. Biochem. 119*, 193−199.
11. Van Raaij, M. J., Orriss, G. L., Montgomery, M. G., Runswick, M. J., Fearnley, I. M., Skehel, J. M., and Walker, J. E. (1996) *Biochemistry 35*, 15618−15625.
12. Lebowitz, M. S., and Pedersen, P. L. (1996) *Arch. Biochem. Biophys. 330*, 342−354.
13. Polgreen, K. E., Featherstone, J., Willis, A. C., and Harris, D. A. (1995) *Biochim. Biophys. Acta 1229*, 175−180.
14. Papa, S., Zanotti, F., Cocco, T., Perrucci, C., Candita, C., and Minuto, M. (1996) *Eur. J. Biochem. 240*, 461−467.
15. Van Heeke, G., Deforce, L., Schnizer, R. A., Shaw, R., Couton, J. M., Shaw, G., Song, P. S., and Schuster, S. M. (1993) *Biochemistry 32*, 10140−10149.
16. Ichikawa, N., Karaki, A., Kawabata, M., Ushida, S., Mizushima, M., and Hashimoto, T. (2001) *J. Biochem. 130*, 687−693.
17. Van de Stadt, R. J., de Boer, B. L., and Van Dam, K. (1973) *Biochim. Biophys. Acta 292*, 338−349.
18. Husain, I., and Harris, D. A. (1983) *FEBS Lett. 160*, 110−114.
19. Power, J., Cross, R. L., and Harris, D. A. (1983) *Biochim. Biophys. Acta 724*, 128−141.
20. Klein, G., and Vignais, P. V. (1983) *J. Bioenerg. Biomembr. 15*, 347−362.
21. Husain, I., Jackson, P. J., and Harris, D. A. (1985) *Biochim. Biophys. Acta 806*, 64−74.
22. Lippe, G., Sorgato, M. C., and Harris, D. A. (1988) *Biochim. Biophys. Acta 933*, 1−11.
23. Lippe, G., Sorgato, M. C., and Harris, D. A. (1988) *Biochim. Biophys. Acta 933*, 12−21.
24. Dreyfus, G., Gómez-Puyou, A., and Tuena de Gómez-Puyou, M. (1981) *Biochem. Biophys. Res. Commun. 100*, 400−406.
25. Beltran, C., Tuena de Gómez-Puyou, M., Gómez-Puyou, A., and Darszon, A. (1984) *Eur. J. Biochem. 144*, 151−157.
26. Lopez-Mediavilla, C., Vigny, H., and Godinot, C. (1993) *Eur. J. Biochem. 215*, 487−496.
27. Gomez-Fernandez, J. C., and Harris, D. A. (1978) *Biochem. J. 176*, 967−975.
28. Cintrón, N. M., Hullihen, J., Schwerzmann, K., and Pedersen, P. L. (1982) *Biochemistry 21*, 1878−1885.
29. Milgrom, Yu. M. (1989) *FEBS Lett. 246*, 202−206.
30. Galante, Y. M., Wong, S.-Y., and Hatefi, Y. (1981) *Biochemistry 20*, 2671−2678.
31. Chernyak, B. V., Sigalat, C., Diolez, P., and Haraux, F. (1995) *Biochim. Biophys. Acta 1229*, 121−128.
32. Hashimoto, T., Negawa, Y., and Tagawa, K. (1981) *J. Biochem. 90*, 1151−1157.
33. Schouppe, C., Vaillier, J., Venard, R., Rigoulet, M., Velours, J., and Haraux, F. (1999) *J. Bioenerg. Biomembr. 31*, 105−117.
34. Horstman, L. L., and Racker, E. (1970) *J. Biol. Chem. 245*, 1336−1344.
35. Satre, M., de Jerphanion, M.-B., Huet, J., and Vignais, P. V. (1975) *Biochim. Biophys. Acta 387*, 241−255.
36. Chan, S. H. P., and Barbour, R. L. (1976) *Biochim. Biophys. Acta 430*, 426−433.
37. Panchenko, M. V., and Vinogradov, A. D. (1985) *FEBS Lett. 184*, 226−230.
38. Khodjaev, E.-Yu., Komarnitsky, F. B., Capozza, G., Dukhovich, V. F., Chernyak, B. V., and Papa, S. (1990) *FEBS Lett. 272*, 145−148.
39. Fujii, S., Hashimoto, T., Yoshida, Y., Miura, R., Yamano, T., and Tagawa, K. (1983) *J. Biochem. 93*, 189−196.
40. Cabezón, E., Butler, P. J. G., Runswick, M. J., and Walker, J. E. (2000) *J. Biol. Chem. 275*, 25460−25464.
41. Cabezón, E., Arechaga, I., Butler, P. J. G., and Walker, J. E. (2000) *J. Biol. Chem. 275*, 28353−28355.
42. Domínguez-Ramírez, L., Mendoza-Hernandez, G., Carabez-Trejo, A., Gómez-Puyou, A., and Tuena de Gómez-Puyou, M. (2001) *FEBS Lett. 507*, 191−194.
43. Hashimoto, H., Yoshida, Y., and Tagawa, K. (1983) *J. Biochem. 94*, 715−720.
44. Hashimoto, T., Yoshida, Y., and Tagawa, K. (1984) *J. Biochem. 95*, 131−136.
45. Matsubara, H., Inoue, K., Hashimoto, T., Yoshida, Y., and Tagawa, K. (1983) *J. Biochem. 94*, 315−318.
46. Yoshida, Y., Wakabayashi, S., Matsubara, H., Hashimoto, T., and Tagawa, K. (1984) *FEBS Lett. 170*, 135−138.
47. Hashimoto, T., Yoshida, Y., and Tagawa, K. (1987) *J. Biochem. 102*, 685−692.
48. Hashimoto, T., Yoshida, Y., and Tagawa, K. (1990) *J. Biochem. 108*, 17−20.
49. Ichikawa, N., Yoshida, Y., Hashimoto, T., Ogasawara, N., Yoshikawa, H., Imamoto, F., and Tagawa, K. (1990) *J. Biol. Chem. 265*, 6274−6278.
50. Cabezón, E., Butler, P. J. G., Runswick, M. J., Carbajo, R. J., and Walker, J. E. (2002) *J. Biol. Chem. 277*, 41334−41341.
51. Hashimoto, T., Yoshida, Y., and Tagawa, K. (1990) *J. Bioenerg. Biomembr. 22*, 27−38.
52. Hong, S., and Pedersen, P. L. (2002) *Arch. Biochem. Biophys. 405*, 38−43.
53. Mimura, H., Hashimoto, T., Yoshida, Y., Ichikawa, N., and Tagawa, K. (1993) *J. Biochem. 113*, 350−354.
54. Paul, M.-F., Velours, J., Arselin de Chateaubodeau, G., Aigle, M., and Guérin, B. (1989) *Eur. J. Biochem. 185*, 163−171.
55. Arselin de Chateaubodeau, G., Guérin, M., and Guérin, B. (1976) *Biochimie 58*, 601−610.
56. Guérin, B., Labbe, P., and Somlo, M. (1979) *Methods Enzymol. 55*, 149−159.
57. Lowry, O. H., Rosebrough, N. J., Farr, A. L., and Randall, R. J. (1951) *J. Biol. Chem. 193*, 265−275.
58. Ebner, E., and Maier, K. (1977) *J. Biol. Chem. 252*, 671−678.
59. Tagawa, K., Hashimoto, T., and Yoshida, Y. (1986) *Methods Enzymol. 126*, 504−512.
60. Smith, P. K., Krohn, R. I., Hermanson, G. T., Mallia, A. K., Gartner, F. H., Provenzano, M. D., Fujimoto, E. K., Goeke, N. M., Olson, B. J., and Klenk, D. C. (1985) *Anal. Biochem. 150*, 76−85.
61. Schägger, H., and Von Jagow, G. (1987) *Anal. Biochem. 166*, 368−379.
62. Arselin, G., Vaillier, J., Graves, P.-V., and Velours, J. (1996) *J. Biol. Chem. 271*, 20284−20290.
63. Beauvoit, B., Bunoust, O., Guérin, B., and Rigoulet, M. (1999) *Eur. J. Biochem. 263*, 118−127.
64. He, X., Miginiac-Maslow, M., Sigalat, C., Keryer, E., and Haraux, F. (2000) *J. Biol. Chem. 275*, 13250−13258.
65. Okada, Y., Hashimoto, T., Yoshida, Y., and Tagawa, K. (1986) *J. Biochem. 99*, 251−256.
66. Ritov, V. B., Tverdislova, I. L., Avakyan, T. Yu., Menshikova, E. V., Leikin, Yu. N., Bratkovskaya, L. B., and Shimon, R. G. (1992) *Gen. Physiol. Biophys. 11*, 49−58.
67. Grivennikova, V. G., Kapustin, A. N., and Vinogradov, A. D. (2001) *J. Biol. Chem. 276*, 9038−9044.
68. Arselin, G., Gandar, J. C., Guérin, B., and Velours, J. (1991) *J. Biol. Chem. 266*, 723−727.
69. Chernyak, B. V., Khodjaev, E. Tu., and Kozlov, I. A. (1985) *FEBS Lett. 187*, 253−256.
70. Ichikawa, N., Nakabayashi, K., and Hashimoto, T. (2002) *J. Biochem. 132*, 649−654.

BI034394T